Planar magnetoinductive lens for three-dimensional subwavelength imaging

M. J. Freire[a] and R. Marqués
Departamento de Electrónica y Electromagnetismo, Facultad de Física, Universidad de Sevilla, Avenida Reina Mercedes s/n, E 41012 Seville, Spain

(Received 5 January 2005; accepted 15 March 2005; published online 28 April 2005)

A planar near-field magnetoinductive lens operating in the microwave range is presented. The proposed device consists of two parallel planar arrays of metallic broadside coupled (BC) split-ring resonators (SRRs), or BC-SRRs. The power coming from a point-like source located in front of the lens is focused into a receiver located in free space beyond the lens. This focus is clearly separated from the back side of the lens, and has a size that is an order of magnitude smaller than the free space wavelength of the incoming field. The imaging properties of the device relies mainly on the excitation of magnetoinductive surface waves on the BC-SRR arrays. By simply scaling the BC-SRRs' size, as well as the arrays periodicity, the operation frequency of the device can be tuned in a wide frequency range. Thus, the proposed design is potentially useful for many applications ranging from megahertz to terahertz. © *2005 American Institute of Physics*.
[DOI: 10.1063/1.1922074]

After the seminal papers of Veselago[1] and Pendry[2] on the imaging properties of left-handed slabs, there has been a great deal of interest on this subject, including the design of subdiffraction imaging devices.[2] In fact, lenses overcoming diffraction limits could find application not only in imaging devices, but also in the recording of information, microwave heating, and many other technological areas. However, it soon became apparent that losses and dispersion—both unavoidable in any practical left-handed material—would strongly limit the performance of these devices.[3–5] In particular, losses will prevent subwavelength imaging at distances higher than a small number of wavelengths in any practical lens.[4,5] Therefore, attention will soon focus in the near-field imaging of electromagnetic signals. In this way, a quasiperfect imaging in the quasielectrostatic limit by using a slab of negative dielectric permitivitty (ε) was proposed in Ref. [2]. Since many metals show this property at optical frequencies, thin metallic slabs could be good candidates for obtaining near-field subwavelength imaging at these frequencies. Quasiperfect near-field imaging can be also obtained by using magnetized ferrite slabs operating in the microwave range.[6]

Practical realizations of subdiffraction imaging devices are currently restricted to the microwave range.[7,8] These realizations make use of planar circuit analogous of left-handed media[7] as well as of very thin (single-cell depth) highly anisotropic left-handed slabs in free space.[8] The first realization[7] does not seem to open the way to any possible generalization leading to three-dimensional practical lenses. The second one, apart from being highly anisotropic, does not enable the reproduction of images "of finite depth,"[8] since the imaging is restricted to planes parallel to the lens. Microwave three-dimensional imaging was already reported in Ref. 9, although the size of the focus was not of subwavelength dimensions. Thus, it can be concluded that devices producing three-dimensional isotropic subwavelength imaging have not been previously reported.

In this letter we present a planar magnetoinductive lens for near-field imaging in the microwave range. As in previous work,[2,6–8] the key concept of the proposed imaging process is the amplification, inside the lens, of the evanescent Fourier harmonics (FHs) coming from the source. This amplification restores the amplitude of each FH at the image plane so that the source field is reproduced at this plane. In negative-ε imaging devices[2] and in magnetized ferrite slabs,[6] this amplification is due to the excitation of surface waves (surface plasmons in metals and magnetostatic surface waves in ferrites) at the shadowed interface of the slab. These surface waves, which decay from this interface towards both the source and the image, are coupled to the decaying evanescent FHs coming from the source in such a way that the amplitude of these FHs is restored at the image plane.[2,6] This mechanism is sketched in Fig. 1(a), where the decaying-growing-decaying process is illustrated for a single FH. (Recently, a similar mechanism of amplification of evanescent modes has been reported in a pair of coupled resonator arrays.[10]) In order to achieve ideal perfect imaging, this process should take place for all the FHs coming from the source. Since the lens operates at a single frequency, it implies that the dispersion relation for the surface waves at the shadowed interface of the lens [the plane $z=0$ in Fig. 1(a)] should be very flat, so that surface waves corresponding to whatever value of the wave vectors (k_x,k_y) can be simultaneously excited at the frequency of operation of the lens.[2,6,10] This condition is actually fullfilled by the ideal surface plasmons supported by a negative-ε slab interface,[2] and by the magnetostatic surface waves supported by a magnetized ferrite slab interface.[6]

In the proposed device (see Fig. 2), magnetoinductive surface waves are excited at the shadowed lens interface. Magnetoinductive waves were first reported by Shamonina *et al.*[11] in both one-, two-, and three-dimensional arrays of split-ring resonators (SRRs). These waves are produced by the inductive coupling between SRRs, due to the strong magnetic dipoles induced at each resonator near its resonance. Magnetoinductive waves behave as quasimagnetostatic sur-

[a]Electronic mail: freire@us.es

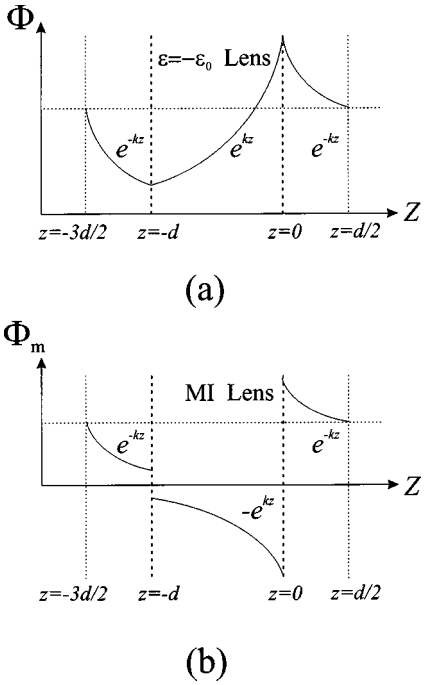

FIG. 1. (a) Decaying-growing-decaying behavior of the electrostatic potential Ψ in the negative-permittivity (ε) lens. (b) Decaying-growing-decaying behavior of the magnetostatic potential Ψ_m in the magnetoinductive (MI) lens.

face waves in many aspects, as it was noted in Ref. 12. The dispersion relation for a planar square array of SRRs as those shown in Fig. 2 can be written as[11,12]

$$\frac{\omega_0^2}{\omega^2} = 1 + 2\frac{M}{L}[\cos(k_x a) + \cos(k_y a)], \tag{1}$$

where only the coupling between the nearest neighbors has been taken into account.[12] In Eq. (1), L and M denote the SRRs' self-inductance and mutual inductance, respectively, and a is the array periodicity. The fractional bandwidth $\Delta\omega/\omega_0$, predicted by Eq. (1) is given by

$$\frac{\Delta\omega}{\omega_0} \approx 4\frac{M}{L}, \tag{2}$$

where $\Delta\omega$ is the bandwidth of the magnetoinductive surface wave excitation. This bandwidth is very small, of the order of a 10% in the configuration shown in Fig. 2. Thus, the dispersion curve of the magnetoinductive waves is almost flat, which is required for subwavelength imaging. Since magnetoinductive waves are quasimagnetostatic waves, the magnetic field $\mathbf{H}$ can be obtained from the quasistatic magnetic potential Φ_m as $\mathbf{H}=-\text{grad}\,\Phi_m$. Since the magnetostatic potential satisfies Laplace's equation in free space, the z dependence for the magnetoinductive waves that can be excited at the SRR square arrays is given by

$$\Phi_m(k_x,k_y,z) = \Phi_{m,0}\exp[\pm k|z - z_0|], \tag{3}$$

where $\Phi_{m,0}$ is a constant, $k=(k_x^2+k_y^2)^{1/2}$, and z_0 denotes the position of each lens interface. According to Fig. 1, the plus sign in Eq. (3) corresponds to $z_0=-d$ and the minus sign corresponds to $z_0=0$. It should be noted that the behavior of Φ_m at both sides of $z=-d$ would be *nonphysical* for an isolated SRR array, since the magnetostatic potential would grow to infinity at both sides of the array. However, the presence of the source at $z=-3d/2$, as well as that of the companion SRR array at $z=0$, allows for the excitation of this field configuration around the SRR array at $z=-d$. Regarding the behavior of Φ_m near the SRR array, it differs from that of surface plasmons and ferrite magnetostatic potentials.[2,6] On the one hand, the magnetostatic potential Φ_m should experience a discontinuity at each lens interface equal to the mean magnetic dipole moment per unit area: $\Delta\Phi_m=N\langle m_z\rangle$ ($\langle m_z\rangle$ is the average magnetic dipole of the SRRs and N is the number of SRRs per unit area). On the other hand, the normal component of the magnetic field (H_z) should be continuous across the lens interfaces. The behavior of Φ_m for the considered magnetoinductive surface waves is shown in Fig. 1(b). Although this behavior differs from that reported in Refs. 2 and 6 for surface plasmons and magnetostatic surface waves, it can still produce FH amplification, as sketched in Fig. 1(b) [It is worth noting that if the magnitude of the magnetostatic potential were plotted, this graphic would be identical to Fig. 1(a).] In Figs. 1(a) and 1(b) it can be seen how a single FH coming from the source (at $z=-3d/2$) is coupled to a surface wave excited at the shadowed lens interface (at $z=0$), and how its amplitude is finally restored at the focus plane ($z=d/2$).

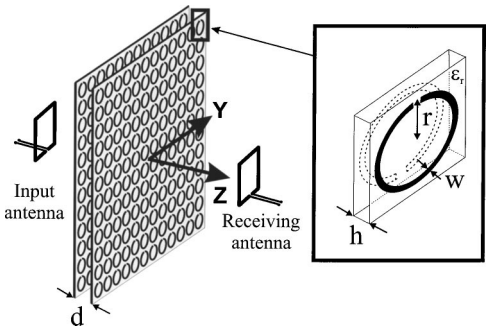

FIG. 2. Experimental setup for the measurement of the reported magnetoinductive microwave lens. The lens consists of two parallel square planar dielectric substrates with an area of 7×7 cm^2, separated by a foam slab of thickness $d=4$ mm. A periodic two-dimensional array of BC-SRRs is photoetched on the two interfaces of each substrate. The square inset in the figure shows in detail the geometry of the BC-SRR, which has an outer radius $r=2$ mm and a ring width $w=0.5$ mm. The periodicity of the array is 5 mm. The dielectric substrate is alumina, which is commonly used in microwave circuits, with thickness $h=0.254$ mm and dielectric permittivity $\varepsilon_r=10$. Input antenna and receiving antenna are placed at the opposite sides of the lens. Both antennas are squared loops with an area of 1×1 cm^2 and are fabricated by photoetching a metallic pattern on an low permittivity substrate. The input antenna is fixed at a certain distance from the left interface of the lens, and the receiving antenna can be scanned along the *Y-Z* directions shown in the figure.

Figure 2 shows the practical device employed in this work. The lens consists of two parallel square arrays of SRRs separated a distance d (a layer of Rohacell™ foam was placed between the layers containing the arrays to achieve mechanical stability). Broadside coupled SRRs (BC-SRRs) are used instead of conventional SRRs in order to avoid cross-polarization effects, and to reduce the electrical size of the resonators.[13] The BC-SRRs are photoetched on a dielectric substrate of thickness h, as is shown in the inset of Fig. 2. Two square loop antennas are used as source and receiver, respectively. These square loops are also fabricated by photoetching a metallic pattern on a dielectric substrate. The size of these loops is taken as four times the unit cell area of the BC-SRRs array in order to average the detailed contribution to the total field coming from each individual resonator. The

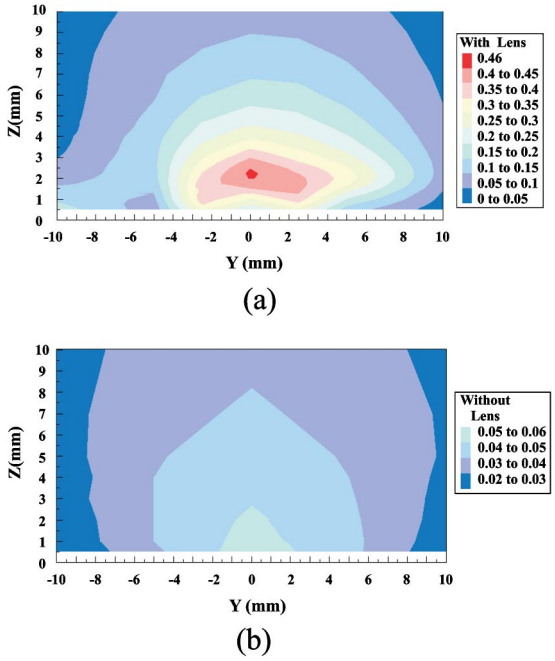

FIG. 3. (Color online) Experimental results obtained with the setup shown in Fig. 2. The data are referred to the magnitude of the transmission coefficient between the input antenna and the receiving antenna with the lens (a) and without it (b). The measurements were carried out by using a Vector Network Analyzer HP 8510 B. The input antenna is fixed at a distance of 2 mm from the left interface of the lens (the location of the left interface corresponds to $z=-3d/2$ in Fig. 1(b) and its operating frequency is 3.23 GHz. The receiving antenna is scanned along the *Y*-*Z* directions shown at the right side of the lens in Fig. 2. Note that in (a) the image is formed at the point $y=0$ mm, $z=2.25$ mm [$z=d/2$ in Fig. 1(b)]; that is at a distance of 2.25 mm from the right interface of the lens. This distance agrees very approximately with the half-width of the lens; i.e., with the sum of the foam half-width (2 mm) and the microwave board thickness (0.254 mm). Therefore, the image formation obeys the proposed theory. Note that in (b) the magnitude of the transmission coefficient in the point $y=0$ mm, $z=2.25$ mm in the absence of the lens is one order of magnitude lower than in the same point when the lens is present.

input antenna (the source) is fixed at a distance $d/2$ from the lens; the output antenna is scanned in the *y*-*z* plane in order to search for the image of the input antenna. Figure 3(a) shows the measured transmission coefficient between both antennas when the lens is present, and Fig. 3(b) shows the measurement when the lens is removed. Figure 3(a) clearly shows that the transmitted power has a maximum at a distance $d/2$ of the shadowed interface of the lens, that is, at a distance $2d$ from the the input antenna, in agreement with the proposed theory. Nothing similar is observed when the lens is absent. The half-intensity width of the maximum is around 10 mm in the lateral direction (*y* axis), and less than 2 mm in the perpendicular one (*z* axis). These distances are smaller than the free space wavelength at the operating frequency (about 100 mm) by one order of magnitude. The intensity of the maximum is indeed remarkable, since it is one order of magnitude higher than the intensity at the same point when the lens is removed. A noticeable fact is that the reported maximum is not located at the lens shadowed interface but clearly removed to the neighborhood of $z=d/2$. Thus, a three-dimensional subwavelength image of the source is obtained. The slight asymmetries of the field patterns shown in Fig. 3 can be attributed to tolerances in the lens fabrication process, or to the positioning device used for scanning the output antenna.

In summary, subwavelength microwave three-dimensional imaging by a flat magnetoinductive microwave lens has been shown. The reported image has a subwavelength size, which is in agreement with the "perfect lens" theory,[2] and is clearly removed from the edge of the lens. An advantage of the reported device over previous near-field lens designs is the simplicity of its manufacturing process, which consists mainly of etching two planar metallic patterns on a conventional circuit board by means of standard microwave circuit manufacturing techniques. For these reasons, we feel that the reported concepts can substantially improve present approaches to electromagnetic imaging devices. Since BC-SRRs are metallic resonators with a linear response, whose frequency of resonance can be tuned by simply scaling their size, the operation frequency of the proposed device can be also tuned in a broad frequency range. This frequency range will be limited mainly by the usefulness of the SRR topology as a practical magnetic resonator design. Since this usefulness seems to have been actually demonstrated up to the terahertz range,[14] the limits of application of the proposed design would also extend at least to these frequencies. In addition to its theoretical interest, devices based on the reported concepts can find practical applications in many technological areas, such as microwave imaging or heating for industrial and health applications.

This work has been supported by DGI, Ministerio de Educación y Ciencia (SPAIN), under project contract no. TEC2004-04249-C02-02.

[1] V. G. Veselago, Usp. Fiz. Nauk **92**, 517 (1967) [Sov. Phys. Usp. **10**, 509 (1968)].
[2] J. B. Pendry, Phys. Rev. Lett. **85**, 3966 (2000).
[3] N. García and M. Nieto-Vesperinas, Phys. Rev. Lett. **88**, 207403 (2002).
[4] D. R. Smith, D. Schurig, M. Rosebluth, S. Schultz, S. Anantha-Ramakrishna, and J. B. Pendry, Appl. Phys. Lett. **82**, 1506 (2003).
[5] R. Marques and J. Baena, Microwave Opt. Technol. Lett. **41**, 290 (2004).
[6] R. Marques, F. Mesa, and F. Medina, Appl. Phys. Lett. **86**, 023505 (2005).
[7] A. Grbic and G. Eleftheriades, Phys. Rev. Lett. **92**, 117403 (2004).
[8] A. N. Lagarkov and V. N. Kissel, Phys. Rev. Lett. **92**, 077401 (2004).
[9] A. A. Houck, J. B. Brock, and I. L. Chuang, Phys. Rev. Lett. **90**, 137401 (2003).
[10] S. Maslowski, S. Tretyakov, and P. Alitalo, J. Appl. Phys. **96**, 1293 (2004).
[11] E. Shamonina, V. A. Kalinin, K. H. Ringhofer, and L. Solymar, J. Appl. Phys. **92**, 6252 (2002).
[12] M. J. Freire, R. Marques, and F. Medina, Appl. Phys. Lett. **85**, 4439 (2004).
[13] R. Marqués, F. Medina, and R. Rafii-El-Idrissi, Phys. Rev. B **65**, 14440 (2002).
[14] S. Linden, C. Enrich, M. Wegener, J. Zhou, T. Koschny, and C. M. Soukoulis, Science **306**, 1351 (2004).